Pergamon

Atmospheric Environment Vol. 30, No. 22, pp. 3715–3731, 1996

PII: S1352-2310(96)00103-3
1352-2310/96 $15.00 + 0.00

WIND TUNNEL SIMULATIONS OF PLUME DISPERSION THROUGH GROUPS OF OBSTACLES

M. J. DAVIDSON,*† W. H. SNYDER,‡ R. E. LAWSON, Jr‡ and J. C. R. HUNT*§

* Department of Applied Mathematics and Theoretical Physics, University of Cambridge, Silver Street, Cambridge CB3 9EW, U.K.; and ‡ Atmospheric Sciences Modeling Division, Air Resources Laboratory, National Oceanic and Atmospheric Administration, Research Triangle Park, NC 27711, U.S.A. On assignment to the National Exposure Research Laboratory, U.S. Environmental Protection Agency

(*First received* 18 *November* 1995 *and in final form* 13 *March* 1996)

Abstract—In this paper we present the results of two wind-tunnel simulations of dispersion from upwind point sources through a large group of obstacles, and compare these with an associated field study (Davidson *et al.*, 1995, *Atmospheric Environment* **29**, 3245–3256). Detailed flow-field and plume concentration data were obtained from simulations at scales of 1:20 and 1:200. With these data we are able to provide experimental confirmation of many of the ideas developed during the field study and to confirm the experimental results obtained in the field. In doing so, we show that the upstream flow-field parameters are the most effective means of scaling the three data sets to achieve broad quantitative agreement.

Measurements and flow visualisation of the flow-field confirm that there are a number of mechanisms influencing the behaviour of a plume as it passes through an obstacle array: in particular the divergence and convergence of streamlines and changes to the structure of the turbulence within the array. However, although the turbulence within the array is shown to be of greater strength and smaller scale than at corresponding locations outside the obstacle array, it is found that there is little change in the transverse diffusivity (and therefore in the lateral plume width).

The concentration data confirm that the divergence of streamlines near the upstream end of the obstacle array has a significant effect on the vertical width of a plume (σ_z). Changes to the structure of the turbulence appear to have little effect, however, since the transverse diffusivities within the obstacle array are unchanged. Thus, the mean lateral spread and decay of mean concentration of the plume with downstream distance resemble that of a control plume; that is, a plume released under identical conditions where the obstacle array is not present. We also confirm that the mean structure of a plume has a Gaussian form as it passes through an array of obstacles. By contrast, concentration measurements with a high-frequency-response detector confirm that the small-scale, high-strength turbulence rapidly mixes the plume internally, dramatically reducing the strength of concentration fluctuations within the plume.

Since the wind tunnel is shown to be an effective means of modelling this type of field situation, with the appropriate scaling, these studies were extended to consider the effects on plume behaviour of changes in source position, array configuration and array height. Copyright © 1996 Elsevier Science Ltd

Key word index: Wind tunnel, obstacle array, flow field, plume dispersion.

1. INTRODUCTION

The transportation and storage of hazardous materials near a large group of buildings, such as those in an industrial estate or a housing complex, creates a potential problem. Should a release of a toxic substance occur, perhaps as the result of an accidental spillage (a vehicle accident) or as the result of a fire at a storage site, it is important that we be able to evaluate the risk to nearby populated areas. Thus we must be able to predict the behaviour of the cloud of toxic material generated by incidents such as these. We currently have sufficient knowledge to incorporate the effects of most factors that influence the dispersion of a toxic plume over level ground, such as the atmospheric conditions, the nature of the release and the properties of the gases (e.g. Pasquill and Smith, 1983).

Most previous research on the effect of buildings on dispersion has concentrated on the problem of flow and dispersion around a single building and to a lesser extent on small groups of buildings. There are a number of reviews in the literature relevant to this work. Hunt (1984) and Hosker (1981) review the flow and dispersion around a single surface-mounted obstacle and, more recently, Hosker and Pendergrass (1987) review flow and dispersion around small groups of buildings. Fackrell (1984) reviews the application of

† Present address: Department of Civil and Structural Engineering, Hong Kong University of Science and Technology, Clear Water Bay, Kowloon, Hong Kong.

§ Present address: Meteorological Office, London Rd, Bracknell, Berkshire RG12 2SZ, U.K.

a number of simple models (including modified Gaussian plume models) to dispersion from point sources around single and small groups of buildings. More complex eddy-diffusivity models of dispersion around two- and three-dimensional obstacles have been developed by Hunt and Mulhearn (1973), Puttock and Hunt (1979) and Turfus (1986). Jerram *et al.* (1995) have shown how the latter approach may be extended to multiple obstacles, but no general formulae have yet been derived.

There have also been a number of wind-tunnel studies of flow and/or dispersion around a single surface-mounted obstacle in a turbulent boundary layer, notably the work of Snyder and Lawson (1994), Snyder (1993), Davies *et al.* (1980), Castro and Robins (1977), Castro and Snyder (1982) and others. The flow and/or dispersion around small groups of obstacles has been investigated by Britter and Hunt (1979), Hunt (1985) and Kim *et al.* (1990). Hosker and Pendergrass (1987) give some insight into the interaction of a small array of obstacles (up to 5) through a series of flow-visualisation experiments. Some idea of the effects of building density and mean height on the dispersion of a plume in an urban centre can be obtained from the study by Jacko *et al.* (1972). They show that the crosswind-average ground-level concentrations increase as the density and mean height increase. Although useful, the work is rather limited as it does not give an overall picture of the plume behaviour and there is no flow field information.

There have been some field investigations around isolated buildings (e.g. Jones and Griffiths, 1984) and at industrial sites where there are typically a small number of large structures surrounded by a number of small structures. The results from the latter experiments are dominated by dispersion around the single largest obstacle. There have also been investigations into plume behaviour in closely spaced building arrays (representing a portion of an urban environment), where secondary flows become significant (street-canyon effects); the study by Cermak *et al.* (1974) is an example. Also there have been experiments on dispersion over and through vegetative canopies, but the sources are usually placed within or above the canopies, not upwind. If, however, we are concerned (as we are in this paper) with dispersion from point sources upwind of a large group of buildings, where the obstacles are sufficiently spaced that secondary flows are not significant, we have little guidance as to what approach to take.

A recent field study by Davidson *et al.* (1995) has given some insight into the behaviour of a plume as it passes through a large group of obstacles. In the field study, and in the wind-tunnel simulations presented here, we have focused on idealised arrays of a simple pattern (equally spaced and similarly sized obstacles) because idealised studies are the best way to develop a general understanding of the overall plume behaviour. This approach is consistent with that generally adopted for the study of flow and dispersion around single and small groups of obstacles.

In the field experiments two array configurations were considered, a staggered configuration and an aligned configuration. Examples of these configurations are shown in Fig. 1. The configurations are fundamentally different as the staggered array diverts flow onto neighbouring obstacles whereas the aligned array presents channels through which the flow can pass. The dimensions of the obstacles were: height (H) 2.3 m, width (W) 2.2 m and breadth (B) 2.45 m. The ratio of the overall width of the array to the height of the array (L_{A_y}/H), the spanwise aspect ratio was 18 and to the overall breadth (L_{A_x}/H), the streamwise aspect ratio was 17. Flow-visualisation and tracer experiments were conducted for each of the two source positions: at one and four building breadths upstream of the centre of the front face of the obstacle array. The source height was half the obstacle height. The main conclusions of the study were that: (1) the mean concentration profiles of the plume retain a Gaussian form as it passes through the obstacle array; (2) there is little effect on the lateral spread and decay of mean concentration of the plume with downstream distance (i.e. they remain similar to those of the control plume); (3) there is an increase in the vertical extent of the plume and (4) the internal structure of plume changes due to increased mixing within the obstacle array. A limited number of flow field measurements indicated that there was a reduction in the mean velocity within the array.

The wind-tunnel simulations presented in this paper extend these field results by: (1) largely confirming the conclusions drawn from the small field data set (there are some differences which are discussed here); (2) considering the problem of scaling data from small-scale experiments to full-scale scenarios; (3) presenting more detailed flow field information; and (4) considering variations in source position, array configuration and array height. Wind-tunnel simulations are an important alternative to full-scale field experiments because of the reduced cost and our ability to vary and control flow-field parameters which are uncontrollable in the field.

2. WIND-TUNNEL SIMULATIONS

The flow field around sharp-edged obstacles is relatively simple to model in a wind tunnel, since the sharp edges define where the flow separates and, hence, providing the ambient flow is fully turbulent and the building Reynolds number is sufficiently high (Snyder, 1992), similarity is maintained. There are, however, limitations because it is not possible to simulate large-scale atmospheric motions in a wind tunnel. Whereas a plume in the atmosphere meanders because there are always eddy motions larger than its width, a plume in a wind tunnel eventually becomes larger than the largest scales of turbulence and ceases

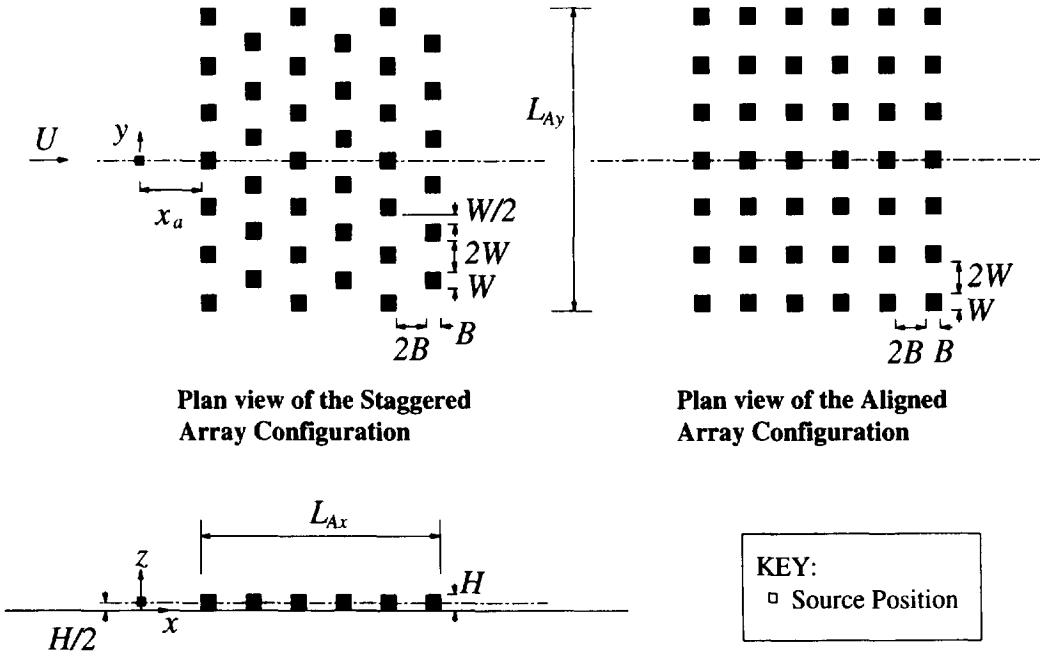

Fig. 1. A schematic diagram of the staggered and aligned obstacle arrays. These configurations were used in the field study and the EPA study. An additional row of obstacles was added to the downstream end of the array for the Cambridge study. Note that x_a is the downstream distance from the source to the front face of the obstacle array and that x is the downstream distance from the source. The quantity $x - x_a$ is therefore the downstream distance from the front face of the obstacle array.

to meander. This is not a serious limitation and much can be gained from studying the simplified wind-tunnel version of the atmospheric problem. The experiments were conducted in two wind tunnels: the United States Environmental Protection Agency's (EPA) wind-tunnel in Research Triangle Park, North Carolina, and the one at the Department of Applied Mathematics and Theoretical Physics, Cambridge, U.K.

The working section of the EPA wind tunnel is 2.1 m high, 3.7 m wide and 18 m long. An atmospheric boundary layer was simulated using the Counihan (1969) system of a fence, vortex generators and downstream gravel roughness. The experiments conducted in this wind tunnel were direct simulations of the field study, but in the wind tunnel detailed flow-field and concentration measurements were made. The staggered array consisted of 39 obstacles with dimensions of $H = W = B = 0.12$ m. This is a scale of approximately 1:20 when compared with the obstacles in the field study. The distance *between* the obstacles was twice the relevant obstacle dimension, that is 0.24 m in both the streamwise (x) and spanwise (y) directions and, therefore, the spanwise aspect ratio was 19 and the streamwise aspect ratio was 16. The aligned array consisted of 42 obstacles of the same dimensions and spacing as the staggered array. These obstacle arrays are shown in Fig. 1.

The wind profile upstream of the arrays was characterised by profile measurements and a reference measurement at a height of $2H$. At this point the ratio of the friction velocity (u_*) to the mean velocity (U) was 0.06 and the roughness height (z_0/H) was 0.0025, both values being comparable to the equivalent full scale values where $u_*/U = 0.07$ at 4 m and $z_0/H = 0.0022$. The wind-tunnel values were estimated from a least-squares fit of the standard logarithmic wind profile formula to the velocity profiles assuming a displacement height (d) of -3 mm (negative because z was measured from the *top* of the gravel roughness). The depth of the boundary layer (L_B) was 0.8 m. The obstacle Reynolds number, based on the obstacle height and the free-stream velocity at that height, was 22,400. Flow-field measurements were made using both an X-array hot-wire anemometer and a pulsed-wire anemometer (Bradbury and Castro, 1971). The use of the hot-wire anemometer was limited to regions outside the obstacle array, because this instrument has poor directional resolution in regions of high turbulence intensity ($> 25\%$) and flow reversals such as those found within the obstacle array. A pulsed-wire anemometer was used to make reliable measurements in these regions. Tracer experiments were conducted using ethane as the tracer gas (ethane is essentially neutrally buoyant in air) and a number of Flame Ionisation Detectors

(FIDs) as sensors. A high-frequency-response FID (Cambustion HFR400) was used to obtain information about the internal structure of the plumes, whereas low-frequency-response FIDs (Beckman 400A) were used to record mean concentration profiles. These experiments are described in a detailed laboratory report by Snyder *et al.* (1991).

The Cambridge wind tunnel has a working section of height 0.45 m, width 0.45 m and length 2.3 m. The limited length of the wind tunnel made it impossible to simulate an atmospheric boundary layer. A turbulent flow field was generated by inserting a square-mesh grid at the inlet to the working section. This grid consisted of 10 mm bars spaced at 114 mm centres. The experiments were then conducted in the natural boundary layer of the wind tunnel. The statistics of this boundary layer were: $u_*/U = 0.05$ at a height of 40 mm, $z_0 = 0.001$ mm, $d = 0$ mm and $L_B = 60$ mm. The smooth nature of the wind tunnel boundary indicates the existence of a viscous sublayer. However, the expected depth of this layer is less than half a millimetre and velocity profiles over the measurement area show no influence from this sublayer. The turbulence intensity in the free stream was 18% near the upstream edge of the obstacle array. Details of the flow field in this wind tunnel using the grid described above are presented by Britter *et al.* (1979). The obstacle width was 10 mm, breadth 10 mm and the height was varied from 10 to 20 mm and finally to 30 mm. The corresponding obstacle Reynolds numbers were 6100, 12,400 and 18,800. Snyder (1992) suggests that the critical Reynolds number for similarity of flow around an obstacle immersed in a simulated atmospheric boundary layer is 4000. The quantitative agreement between the three data sets presented here suggests that a Reynolds number of 6100 was adequate for similarity in this case. The obstacle arrays were approximately 1:200 scale versions of the field study. Flow-field measurements were made upstream and downstream of the arrays with a hot-wire anemometer. No flow-field measurements were made within the arrays. Detailed vertical and horizontal mean concentration profiles were recorded, using ethane as the tracer gas and a FID (Cambustion HFR400) for the sensor.

The ratio of H/L_B varies from 1/6 to 1/2 in the Cambridge wind-tunnel experiments. In the EPA experiments this ratio was 1/7, and in the field study it was approximately 1/250. Due to the different methods of generating the boundary layers in the wind tunnels and the differences in the ratios of the heights of the obstacles to the depth of the boundary layers, we would expect differences in the shear gradients and variations of turbulence intensity over the heights of the obstacle arrays. In the atmospheric boundary layer and the EPA simulated atmospheric boundary layer, the turbulence intensity will decrease with height as the shear gradients decrease, but the boundary layers are in equilibrium, that is, independent of downwind distance. In the Cambridge experiments, the turbulence is grid-generated and, therefore, the turbulence intensity will be relatively uniform throughout any cross-section and decay with downwind distance. The shear gradients over the obstacle height will be much greater in the field study than in either of the wind-tunnel studies, since the obstacle height represents a smaller portion of the overall height of the boundary layer. We have already mentioned the inability of wind tunnels in simulating the large-scale motions present in the atmosphere. In order to quantify the effects of these differences in the flow fields on the behaviour of the plumes, the field-study experiments have been repeated in both the EPA and the Cambridge wind tunnels.

Additional experiments were conducted in the EPA wind tunnel to examine the effects of source position and array type. In the Cambridge wind tunnel, we considered changes in the overall height of the array; changes in the density of the array (by doubling the spacing between the obstacles in the y direction) and differences between the aligned and staggered configurations. The arrays in the Cambridge wind tunnel had an additional row of obstacles downstream of the original arrays (Fig. 1) and with the standard spacings of $2W$ and $2B$, this increased the number of obstacles to 46 for the staggered array and 49 for the aligned array. The overall width and breadth of these arrays were then 0.19 m. When the spacing in the y direction was doubled (to $4W$) the overall width of the array was 0.21 m because the number of obstacles was reduced to 32 for the staggered array and 35 for the aligned array.

3. RESULTS

3.1. *Flow field*

The most important quantities for the purpose of interpreting the dispersion measurements are the mean velocity and the turbulence scales and intensities. The point measurements made in the field study indicate that the mean velocity is reduced within the staggered array to approximately 50% of the upstream value at the same height. During the EPA experiments, detailed mean velocity measurements were made within the staggered and aligned arrays. Figure 2 shows a series of vertical profiles of mean velocity (u-component) recorded along the x-axis of the staggered array. The velocity profiles within the array are clearly not logarithmic and this indicates that application of a change-of-roughness argument to this type of problem would be incorrect.

A more complete picture of the mean flow field can be obtained by considering lateral profiles of velocity. Figure 3 shows lateral profiles of the u-component of the mean velocity at $z = H/2$. The individual effects of the obstacles are seen in the near wakes and an overall reduction in magnitude of the velocity within the array is also observed. The far-wakes of individual

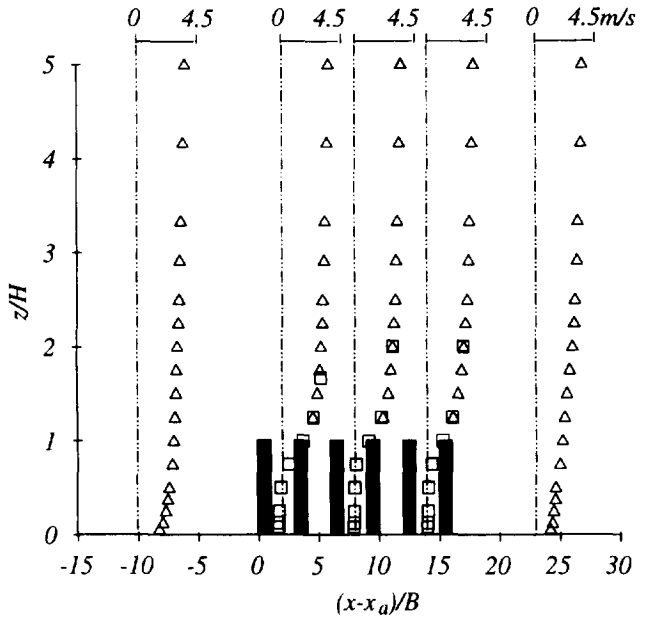

Fig. 2. Vertical profiles of the u-component of mean velocity measured along the x-axis of the staggered obstacle array [EPA]. Data measured with: □, pulsed-wire anemometer; △, hot-wire anemometer. The shaded areas represent the buildings, but the vertical scale is greatly exaggerated.

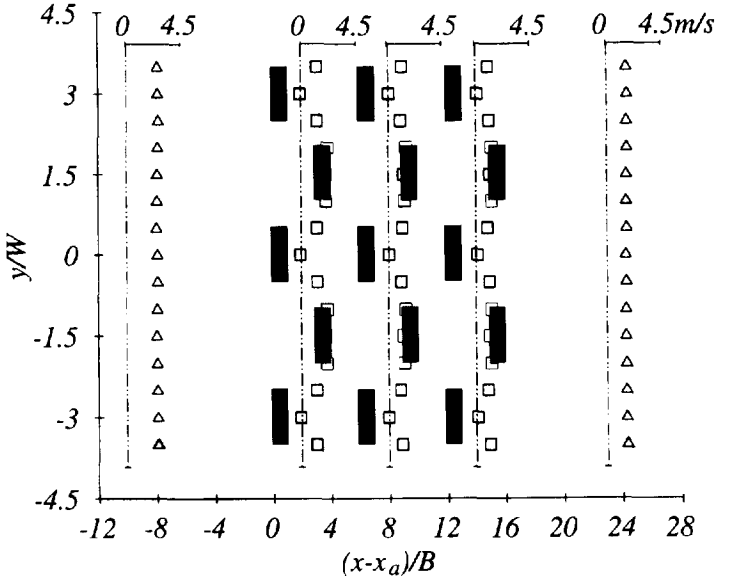

Fig. 3. Lateral profiles of the u-component of mean velocity measured at $z = H/2$, with the staggered obstacle array [EPA]. Data measured with: □, pulsed-wire anemometer; △, hot-wire anemometer. The lateral (y-direction) scale is exaggerated.

obstacles spread and merge with those of neighbouring obstacles, reducing the mean flow through the array. The individual effects of the obstacles quickly decay downstream of the obstacle array; however, an overall reduction in the mean velocity appears to persist for some distance downstream. The data confirm that there is a significant reduction in the mean velocity within the array.

A similar set of profiles is shown in Fig. 4 for the aligned array configuration. The near-wakes of the obstacles are again apparent and the flow can be observed passing down the channels created by the rows of obstacles. The magnitude of the velocity in these channels is less than the corresponding upstream values and, hence, there is an overall reduction in the velocity within the array. The lateral profiles

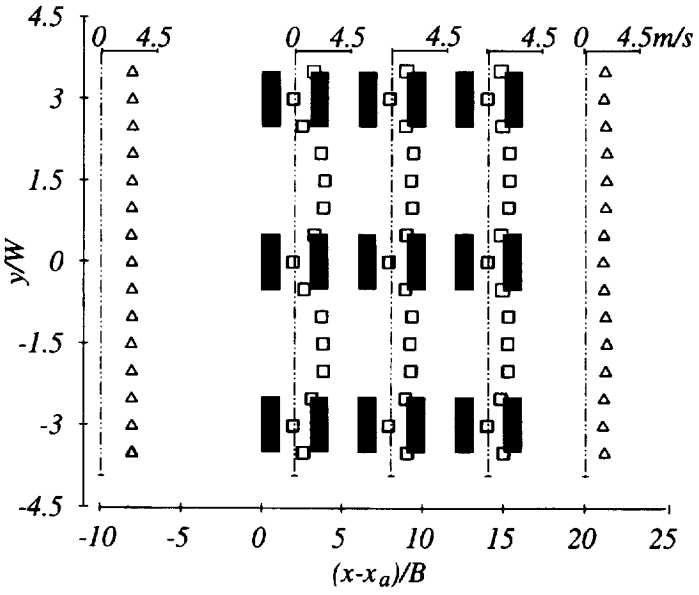

Fig. 4. Lateral profiles of the u-component of mean velocity measured at $z = H/2$, with the aligned obstacle array [EPA]. Data measured with: □, pulsed-wire anemometer; △, hot-wire anemometer. The lateral (y-direction) scale is exaggerated.

were averaged, within the array, in the y-direction to produce spatial and temporal average of velocities at the source height. These horizontally-averaged velocities are presented for both the staggered and aligned arrays in Fig. 5 along with the point measurements from the field study. The mean velocity is reduced to approximately 45% of the upstream value. The region in which the obstacle array influences the flow field (defined as more than a 5% reduction in mean velocity) extends from $\sim 6B$ upstream of the front edge of the array to $\sim 30B$ downstream from the rear edge of the array. The velocity decays rapidly upstream of and within the first 3 rows of the array, but the corresponding recovery occurs more slowly downstream of the array.

The turbulence in the flow field can be characterised by estimating the root-mean-square (r.m.s.) values of the velocity fluctuations (σ_u, σ_v, σ_w) and the integral length scales (L_{11}, L_{22}, L_{33}), in the streamwise direction, of the velocities u, v and w. The temporal resolution of the pulsed-wire anemometer is inadequate for estimating the length scales from time series data and the hot-wire anemometer was used instead. Because of the limitations of the hot-wire anemometer described in Section 2, measurements within the obstacle array could only be made in regions where the turbulence intensities were relatively low and there were few flow reversals (determined by examining the pulsed-wire signal). The turbulence intensities measured by the hot-wire anemometer at these locations ranged from $\approx 25\%$ to $\approx 30\%$. Comparisons of these data with those from the pulsed-wire anemometer, at the same locations, indicated that the hot-wire anemometer was over estimating the intensities within the obstacle arrays by up to 5%. These hot-wire anemometer data must therefore be treated with some caution.

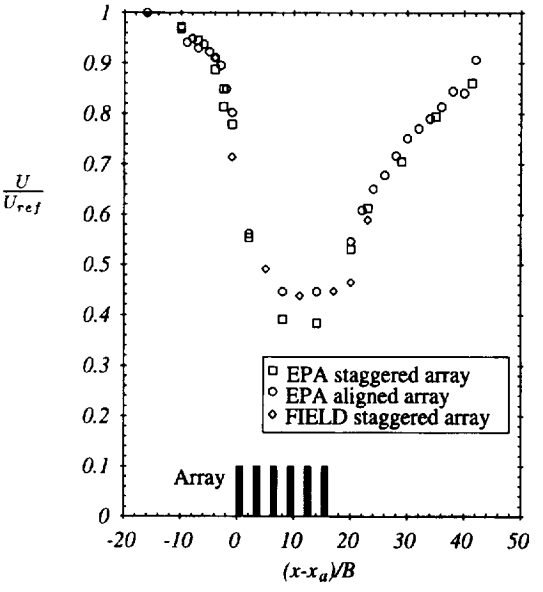

Fig. 5. Spatial (y-direction) and temporal average of the u-component of mean velocity measured at $z = H/2$, with the staggered and aligned obstacle arrays. U_{ref} is the magnitude of the velocity at $(x - x_a)/B = -16$.

The data from time series recorded at a height of $H/2$ are shown in Table 1, for the staggered array ($(x - x_a) = 9.5B$, $y/W = 0$) and the aligned array ($(x - x_a) = 8B$, $y/W = 1.5$). These point measurements indicate the order of the parameters within the

Table 1. Turbulence statistics measured at $x - x_a = 9.5B$, $y = 0$ and $z = H/2$ for the staggered array and $x - x_a = 8B$, $y = 1.5W$ and $z = H/2$ for the aligned obstacle array

	No array	Staggered array	Aligned array
U (m/s)	2.50	1.44	1.66
σ_u (m/s)	0.390	0.397	0.516
L_{11} (m)	0.130	0.037	0.080
K_x (m^2/s)	0.051	0.015	0.041
T_u^L (s)	0.333	0.093	0.156
σ_v (m/s)	0.270	0.356	0.294
L_{22} (m)	0.062	0.050	0.032
K_y (m^2/s)	0.017	0.018	0.009
T_v^L (s)	0.230	0.140	0.109
σ_w (m/s)	0.206	0.270	0.263
L_{33} (m)	0.033	0.029	0.023
K_z (m^2/s)	0.007	0.008	0.006
T_w^L (s)	0.160	0.107	0.087

Note: Data were also recorded in the absence of the obstacle arrays at the same height for comparison [EPA].

obstacle arrays. Data recorded at a similar position when the obstacle arrays were not present are also shown for comparison. The integral length scales were calculated using the formula described in Davidson *et al.* (1995).

Estimates of eddy diffusivities (K_x, K_y, K_z) and Lagrangian time scales (T_u^L, T_v^L, T_w^L) are also shown. The diffusivities are calculated as the product of the relevant length scale and r.m.s. velocity. The Lagrangian time scale is calculated as the length scale divided by the r.m.s. velocity; an estimate that is often satisfactory in inhomogeneous anisotropic flows such as this.

The data suggest that the scale of the turbulence is reduced by the presence of the obstacles. These new scales will be some function of the scale of the obstacles (as the turbulent eddies are shed from these obstacles) and their spacings. The differences in the lateral and vertical eddy diffusivities (K_y, K_z) between the control or no-array case and the staggered array are small and this suggests that the reduction in the scale of the turbulence by the presence of the obstacles is balanced by a corresponding increase in the magnitude of the fluctuations. The dispersion of the plume within the array will therefore be similar to that of the control plume, that is, a plume released under identical conditions when the obstacle array is not present. In the aligned case the lateral eddy diffusivity is reduced and thus the dispersion of the array plume in the lateral plane is inhibited [this was referred to as *channelling* by Davidson *et al.* (1995)]. There is also a change in the longitudinal eddy diffusivity (K_x); this would be significant if we were concerned with a cloud of pollutant passing through the obstacle array, but with continuous releases this result has little relevance. The reductions in the Lagrangian time scales of the turbulence within the array indicate the presence of smaller scale and higher intensity turbulence, which is consistent with the thoroughly-mixed plume structure noted by Davidson *et al.* (1995).

The data presented above give an indication of the effects that an obstacle array which presents a low flat aspect to the oncoming wind has on the flow field. The obstacles exert a drag force on the ambient flow and thus the mean velocity is reduced within the array. This reduction in mean velocity suggests (by continuity) that, near the upstream edge of the array, a portion of the oncoming flow is diverted around the array as a whole. The amount diverted (and the magnitude of the reduction) is dependent upon the density of obstacles within the array. With low flat arrays such as these, the majority of the diverted flow will pass over the top of the array, as opposed to passing around its sides. If, however, we were to increase the height of the obstacles within the array (decreasing L_{Ay}/H and L_{Ax}/H), an increasing portion of the diverted flow would pass around the sides of the obstacle array. If we continued to increase the height of the obstacles, we would eventually reach the two-dimensional limit, where all of the diverted flow passed around the sides of the array, as opposed to passing over the top. Near the downstream edge of a low flat obstacle array, the reverse must occur and fluid will move from above the array down behind the last row of obstacles, as the flow field begins to recover. Figure 5 suggests that the changes downstream of the array occur relatively slowly when compared with the changes at the upstream end.

The mean flow field in proximity to an obstacle array can be divided into a number of regions as shown in Fig. 6. Region I represents the area where the mean velocity and turbulence statistics are unaffected by the presence of the array. In Region II, the streamlines are diverging as a portion of the fluid passes over the array and as the fluid passing into the array decelerates. There is a dividing streamline (surface or tube in the three-dimensional case) above which the fluid passes over the array and below which the fluid passes through it. In Region III, the fluid is moving through the array at a reduced speed; it has a turbulence scale that is some function of the obstacle dimensions and an increased fluctuation strength. Region IV, just above the obstacles, represents a region of strong shear, where a second turbulent boundary layer is developing. In Region V the streamlines gradually converge as the fluid accelerates behind the obstacle array.

Given this classification of the flow around a large group of obstacles, it appears that there are two mechanisms that will influence the behaviour of a plume: the divergence and convergence of streamlines and changes to the nature of the turbulence. The effects on the plume are quite different as diverging or converging streamlines alter the extent of the plume, but there is not necessarily a corresponding change in dilution; whereas changes to the turbulence affect entrainment and, hence, both the extent and dilution of the plume. As an example, consider a tracer released in

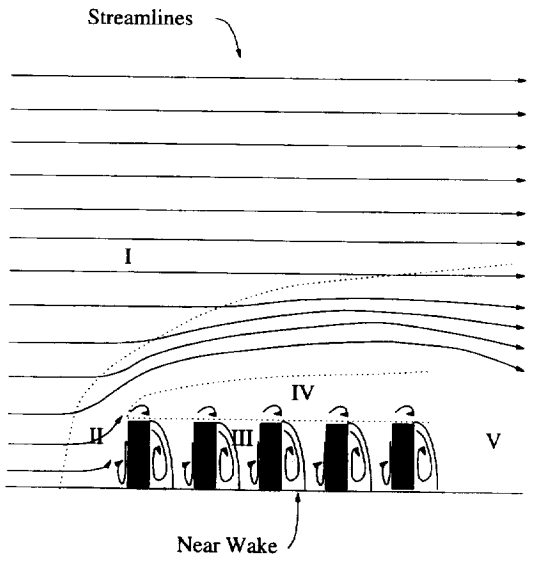

Fig. 6. A schematic diagram of the flow field around a large group of obstacles.

Region I (Fig. 6) and entering the diverging flow in Region II. Because we have one source and no sinks, the flux of tracer downstream from the source is conserved. Therefore, as the fluid decelerates in the diverging flow, the plume must spread more rapidly to maintain a constant tracer flux, but this does not affect the rate of dilution of the plume. Conversely, an increase in the rate of spread of a plume in uniform flow as the result of increased turbulent mixing, must have a corresponding increase in the rate of dilution to maintain the flux of tracer.

The divergence and convergence of the streamlines affects the structure of the turbulence and therefore both types of change occur simultaneously. The rapid divergence of the streamlines near the upstream edge of the array suggests that this may be dominant in Region II. Thus as the plume passes the array, a portion will pass over the array and the remainder will pass through it. The position of the source will have a significant effect on the proportions of the plume entering the different regions. A release above the dividing streamline will result in a larger portion passing over the array, whereas a release below this streamline will result in more material passing through the array. In Region V at the downstream edge of the array, the converging streamlines will act to reduce the extent of the plume. However, the streamline convergence downstream occurs at a slower rate than the divergence near the upstream edge, and the changes in the structure of the turbulence downstream of the obstacle array may dominate the behaviour of the plume in this region. Within the array it appears that, despite the changes in the scales and intensities of the turbulent fluctuations (which changes the internal structure of the plume), the effect on the transverse eddy diffusivities is small; hence, the rate of dilution of the plume with downstream distance is unchanged.

3.2. *Dispersion*

3.2.1. *Scaling and general results.* Experiments on plume dispersion through a staggered array of obstacles have been conducted on three scales (1:1, 1:20, 1:200) and, to make quantitative use of the wind-tunnel data, an effective means of scaling the data is required. The standard approach to scaling data from dispersion influenced by an obstacle's *wake* is to use an obstacle dimension as the relevant length scale (Hosker, 1981). It is assumed that the turbulent eddies shed from the obstacles are dominant with respect to plume dispersion. This is not the relevant scale for a plume impacting *onto* an obstacle (Hunt, 1985). In the problem considered here, where the plume impacts onto a group of obstacles, dispersion is affected both by the upwind atmospheric turbulence and by the wake turbulence. Nevertheless, as a working hypothesis it is assumed that in this case the relevant parameters for defining the dispersion are those of the upwind turbulence, namely the length scales (L_{22}, L_{33}) and the intensity of the fluctuations relative to the mean flow (σ_v/U and σ_w/U) at the source height. These parameters are presented for each of the data sets in Table 2. It was not possible to measure all of these quantities in the Cambridge wind tunnel; however, we were able to establish that $\sigma_u/U = 0.2$ and $L_{11} = 14$ mm at the source height from hot-wire measurements. As the turbulence is grid-generated and, therefore, a reasonable approximation to an isotropic flow field, we can assume that $\sigma_v = \sigma_u$ and that $L_{22} = L_{11}$. The proximity of the boundary suggests that the vertical length scale L_{33} is determined by the distance from the boundary and that was 5 mm. The value of the vertical fluctuation intensity (σ_w/U) at the source height was determined by considering the consistency between the control plume data from the experiments at three different scales and it is assumed to have a value of 0.1.

The wind-tunnel data have been analysed by fitting (using a least-squares routine) Gaussian curves to the profiles of mean concentration (c) data. This method enables us to describe the behaviour of the plume with four parameters, the centreline (maximum) mean concentration (C); the height from the boundary to the peak mean concentrations of each of the two Gaussian distributions, which are commonly combined to describe the vertical profiles as a *reflected* plume (z_{ss}); the lateral spread (σ_y) and the vertical spread (σ_z) of the plume. The addition of z_{ss} and σ_z yields the maximum height of the plume (σ_{Tz}). The Gaussian formula that were applied to the data sets are listed in Davidson *et al.* (1995). In analysing the field data, it was assumed that the value of z_{ss} and the source height (z_s) were the same, because of the close proximity of the source to the positions where profiles were measured. Initially, this assumption was relaxed in analysing the wind-tunnel data. Although there was a tendency for the value of z_{ss} to increase over the array and to decline in the control plume, the

Table 2. Upstream turbulence statistics, at the source height, for the three data sets

	EPA	FIELD	CAMB
σ_u/U	0.156	...	0.2
σ_v/U	0.108	0.3	0.2
σ_w/U	0.082	0.1	0.1
L_{11} (mm)	130	...	14
L_{22} (mm)	62	3000	14
L_{33} (mm)	33	600	5

Note: These statistics were used to scale the data to achieve quantitative agreement between the data sets.

variations were small and therefore the original assumption seems reasonable. The data presented in this paper have been analysed assuming that $z_{ss} = z_s$.

Examples of the vertical and horizontal profiles, recorded in the staggered array, are shown in Figs 7 and 8. The data have been recorded at the three scales and at a number of positions downstream from the source. Gaussian profiles are also shown for comparison. In Fig. 7 the horizontal profiles are Gaussian and self-similar. In Fig. 8 the profiles have a reflected-Gaussian form, however, they are not self-similar when σ_z/z_s is of order 1, and this was generally the case in the experiments. The figures demonstrate that these plumes can be adequately described with Gaussian plume formulae.

In Figs 9–11 the variations of the Gaussian parameters with travel time from the source ($T = x/U$) are presented. The position of the source relative to the obstacle array varies from $1B$ to $12B$. Data from a transformed Gaussian plume model (Pasquill and Smith, 1983), modelling the control plume, are shown for comparison. In Fig. 11, data from the model are presented for two cases: when the ratio of the source height (z_s) to L_{33} is 1, which was the case in the CAMB experiments and when this ratio is 2, which was the case in the FIELD and EPA experiments. The data in these figures are presented using both the traditional approach to scaling (a) and the alternative approach suggested here (b). Clearly, the alternative approach to scaling is superior for the control plume data, because there is quantitative agreement between all three data sets. This is expected because the obstacles were not present in the control plume experiments and therefore the obstacle dimensions should not be relevant when the data is scaled. The agreement between the data sets suggests that the effects of differences in the flow fields on plume dispersion are small for these experiments at the different scales.

The alternative approach also appears to be superior for scaling the array-plume data, although there are some small differences in array-plume behaviour in the Cambridge wind-tunnel and this may be due to the grid-generated flow field. The agreement between the FIELD and the EPA array plume data (under upstream parameter scaling) suggests that the influence of the obstacle dimensions on the turbulence scales is not significant. However, the relevance of the upstream parameters is probably due to a significant

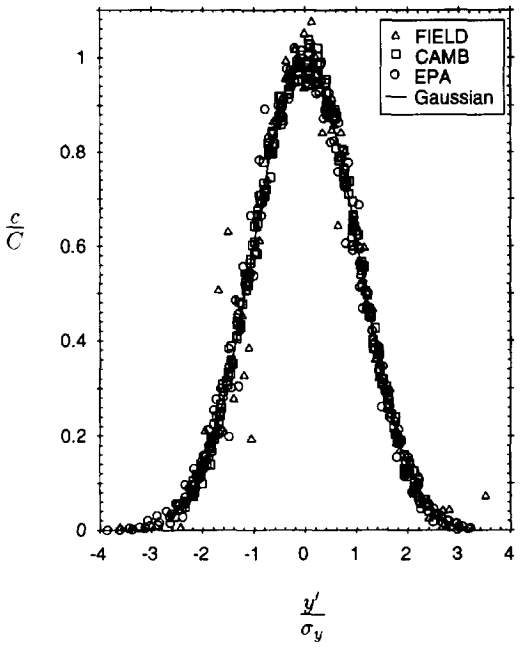

Fig. 7. Horizontal mean-concentration profiles from plumes passing through the staggered array. Data have been recorded at a number of positions downstream of the source and from experiments at the three scales (FIELD, EPA and CAMB). Note: $y' = y - y_{cl}$ and y_{cl} is the distance to the centreline of the plume.

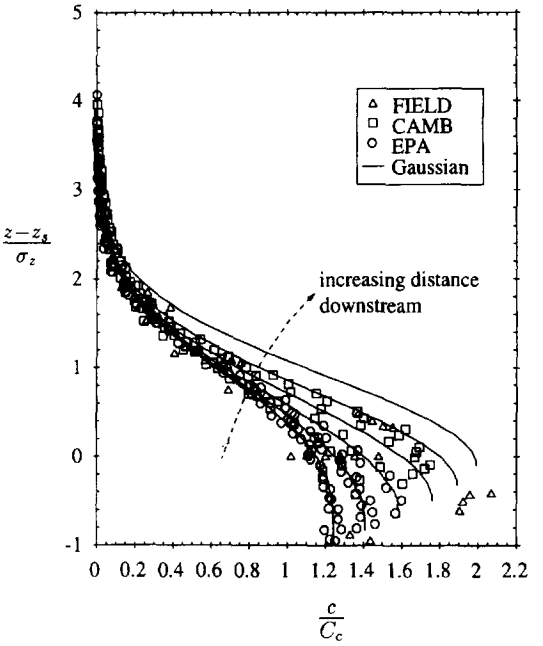

Fig. 8. Vertical mean-concentration profiles from plumes passing through the staggered array. Data have been recorded at a number of positions downstream of the source and from experiments at the three scales (FIELD, EPA and CAMB). Note: $C_c = C/[1 + \exp\{-2(z_s/\sigma_z)^2\}]$.

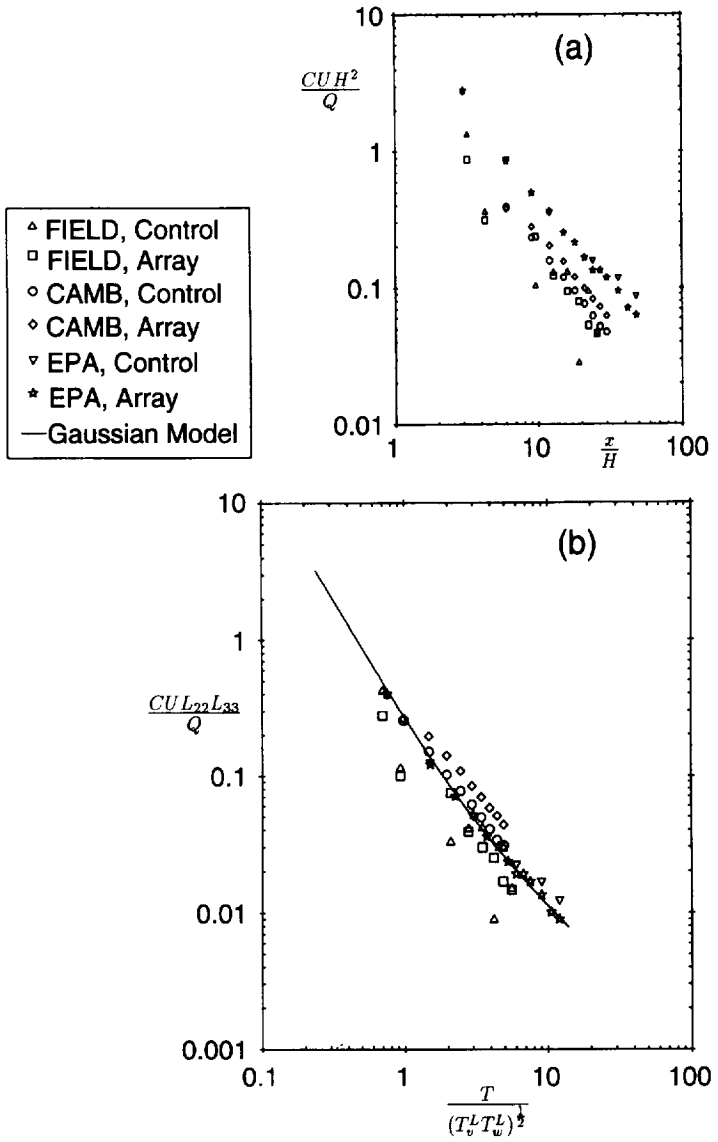

Fig. 9. The decay of mean concentration (at $z = H/2$, $y/W = 0$) with downstream distance of plumes passing through the staggered obstacle array. This figure includes control and array plume data from experiments at the three scales.

portion of the plume passing over the obstacles (as the streamlines diverge) and interacting with the upstream scales in the region above the array. The obstacle dimensions may be more relevant for very tall obstacles, where the plume passes into a flow field that is completely dominated by the obstacle scales.

The results show that these types of field situations can be modelled effectively in a wind tunnel with a simulated atmospheric boundary layer (EPA) and that useful results can be obtained in a small wind tunnel, such as the Cambridge one. The results also confirm the conclusions drawn from the limited field data set.

The main conclusions are that an array causes a significant increase in the vertical height of the plume, but that there is little change in the lateral spread or decay of mean concentration with downstream distance. This suggests that it is the divergence of the streamlines caused by the array as a whole that is the dominant mechanism in determining the dispersion of plumes from upwind sources. This is consistent with the flow field measurements which indicated that changes in the transverse eddy diffusivities were small. However, the instantaneous flow pattern and dispersion within the array is quite different from that over level ground. This is demonstrated by the tracer measurements with the high-frequency-response FID, which confirmed that there is a dramatic reduction in the strength of concentration fluctuations within the arrays. The probability density function of these fluctuations is also changed (compared with the control plumes) and can be modelled effectively

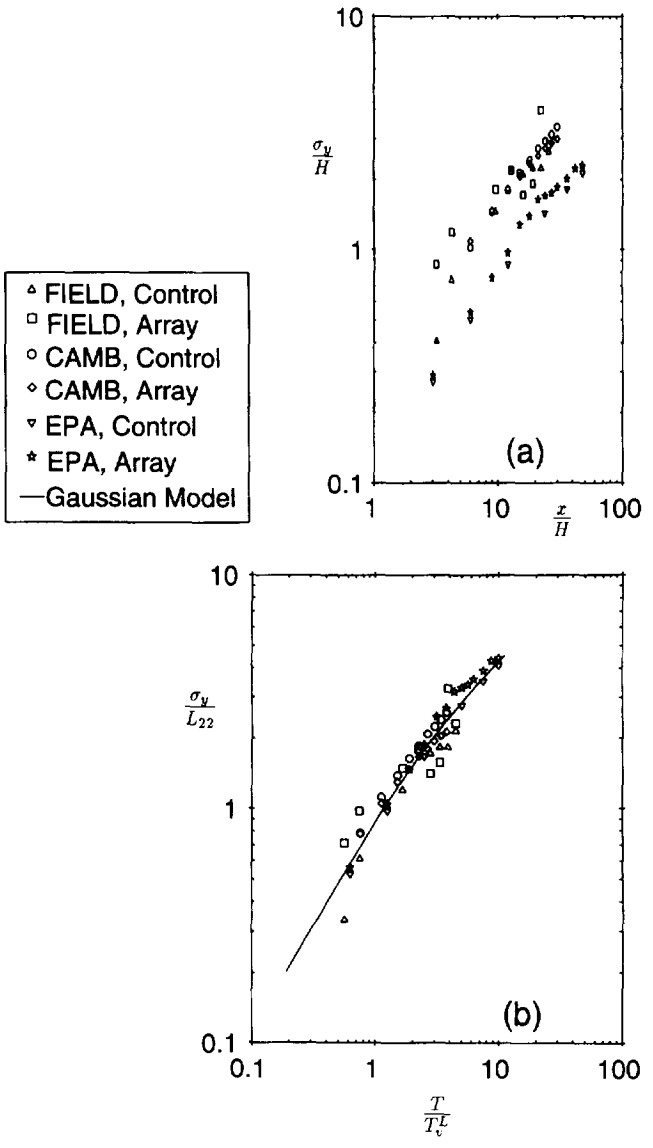

Fig. 10. The lateral growth (at $z = H/2$) of plumes passing through the staggered obstacle array. This figure includes control and array plume data from experiments at the three scales.

with a clipped-normal function (Davidson *et al.*, 1995).

3.2.2. *Array configurations and obstacle dimensions.* Despite small quantitative differences between the array-plume data from the Cambridge study and those from the EPA and FIELD studies, the results from the three sets of experiments are reasonably consistent. The Cambridge study was extended to consider changes in the array configuration and the height of the obstacles. The results of this study give some insight into the importance of these array parameters in determining the behaviour of a plume passing through an obstacle array. Experiments were conducted with the staggered and aligned array configurations. The dimensions of the obstacles were $H = 20$ mm, $W = 10$ mm and $B = 10$ mm, the spacing between them was $2W$ in the spanwise and $2B$ in the streamwise direction, and the streamwise and spanwise aspect ratios were 10. The spacing in the spanwise direction was subsequently increased to $4W$ and the number of obstacles reduced to create two new arrays with streamwise and spanwise aspect ratios of 10. The tracer gas was released $7B$ upstream of the centreline of the array at a height of $H/2$. The behaviour of a plume passing through each of the four arrays was then compared with the behaviour of a control plume released from the source with no array present.

Since scaling in these experiments is not as critical, because the upstream flow field conditions are identical, for simplicity we revert to the traditional form of scaling in presenting the results of these experiments in Figs 12–14. CONT represents the control plume; STG2 represents the staggered array with spacing

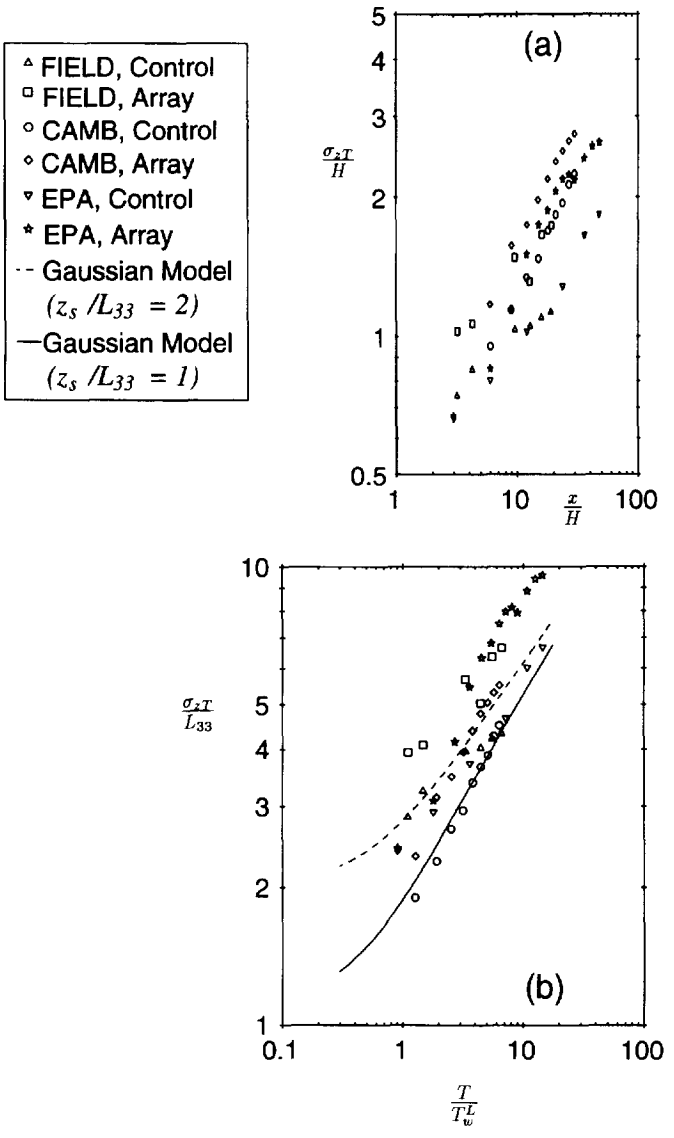

Fig. 11. The vertical extent (at $y/W = 0$) of plumes passing through the staggered obstacle array. This figure includes control and array plume data from experiments at the three scales. Note z_s is the source height.

between the obstacles of $2W$ and $2B$, and ALG2 represents the aligned array with the same spacings. STG4 represents the staggered array with spacings of $4W$ and $2B$ and ALG4 represents the aligned array with the same spacings. The centreline mean concentration (at the source height) of all the array plumes is higher than that of the control plume (Fig. 12). This was observed consistently throughout the Cambridge study and at times in the field study, but it was not evident in the EPA study. The Cambridge results suggest that within the arrays the eddy diffusivities are reduced relative to the upstream values, that is, the reduction in the scales of the turbulence is not balanced by a corresponding increase in the fluctuation strength (this differs from the results of the EPA study — see Section 3.1).

In addition, the *channelling* effect discussed in Davidson *et al.* (1995) is evident in the ALG2 data. The lateral growth of the plume is limited by the presence of rows of obstacles at $y/W = \pm 2.5$ (Fig. 13) and, consequently, the levels of concentration within the array are higher than in all other cases considered. The channelling effect is not evident in the ALG4 array since the plume does not reach the neighbouring rows of obstacles before leaving the array. Apart from channelling, the effects of the arrays on the lateral spread of the plume are small; although the spread is generally larger in the presence of the arrays, at least initially. There are notable changes in the vertical heights of the array plumes when compared with the control plume (Fig. 14). The least affected is the ALG4 array and the most affected is the STG2

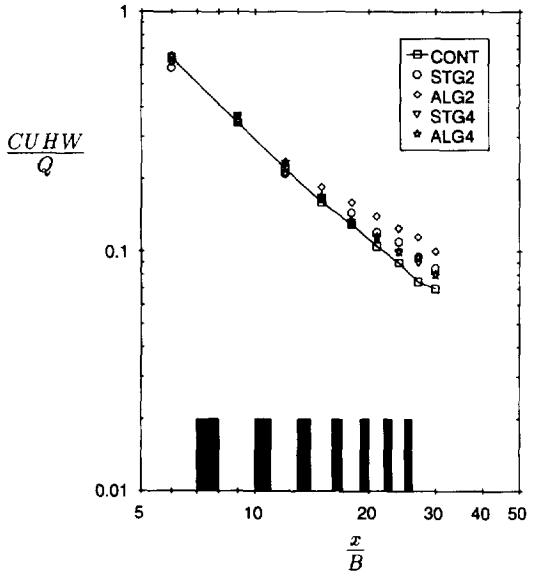

Fig. 12. The effects of different array configurations on the decay of mean concentration (at $z = H/2$, $y/W = 0$) with downstream distance of a plume passing through the arrays [CAMB].

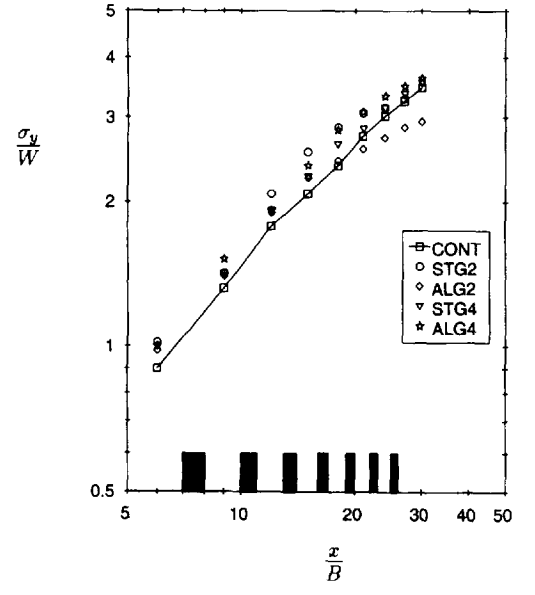

Fig. 13. The effects of different array configurations on the lateral growth (at $z = H/2$) of a plume passing through the arrays [CAMB].

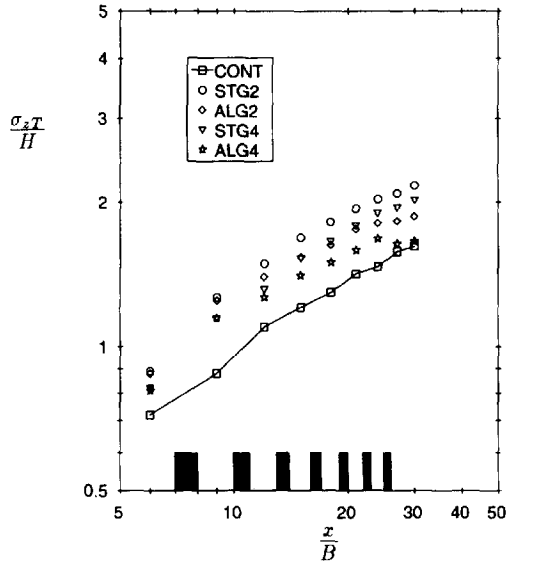

Fig. 14. The effects of different array configurations on the vertical extent (at $y/W = 0$) of a plume passing through the arrays [CAMB].

array, with the ALG2 and STG4 arrays lying in between. This is consistent with the *effective gap* between the obstacles, that is, the distance between the obstacles as they would appear to an upstream observer. The effective gaps being STG2 = $0.5W$, STG4 = $1.5W$, ALG2 = $2W$, and ALG4 = $4W$. It appears, then, that it is this effective gap that influences the divergence of the streamlines (and hence the vertical extent of the plume) rather than the obstacle spacing and that channelling is the only notable difference between the staggered and aligned array configurations.

Experiments were also conducted to investigate the effect of changes in the height of the obstacles on the behaviour of the plume. The staggered array configuration with spacings of $2W$ and $2B$ was used and the height of the obstacles was increased from 10 mm (cubes) to 20 mm and finally to 30 mm. These arrays are denoted as SA10, SA20 and SA30, respectively. The corresponding spanwise aspect ratios were 19, 10 and 6, but we would not expect the results to be sensitive to this ratio as these changes are unlikely to affect the three-dimensional nature of the mean flow. Increasing the obstacle height increases the height of the dividing streamline and also increases the depth of the region over which the obstacles can influence the dispersion of the plume. The source was $7B$ upwind of the arrays at a height of $H/2$ (5 mm).

To emphasize the effects of the obstacle height on the behaviour of the plumes, we use the alternative method of scaling when presenting the results of these experiments in Figs 15–17. As the height of the obstacles increases, the vertical height of the plume also increases, but the results appear to be approaching a limit with the SA20 and SA30 data being very similar (Fig. 17). The centreline mean concentration (at the source height) within the arrays is greater than that of the control plume in all cases, although this increase is not monotonically related to changes in the obstacle height (Fig. 15). The pattern of the lateral spread data, likewise, does not reflect a monotonic relationship (Fig. 16). Changing the height of the obstacles changes the relative importance of streamline divergence and the structure of the turbulence to the

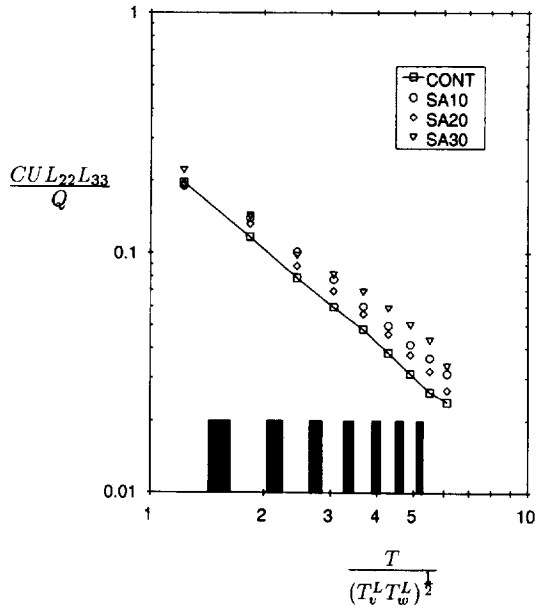

Fig. 15. The effects of changes in the array height on the decay of mean concentration (at $z = H/2$, $y/W = 0$) with downstream distance of a plume passing through the staggered array [CAMB].

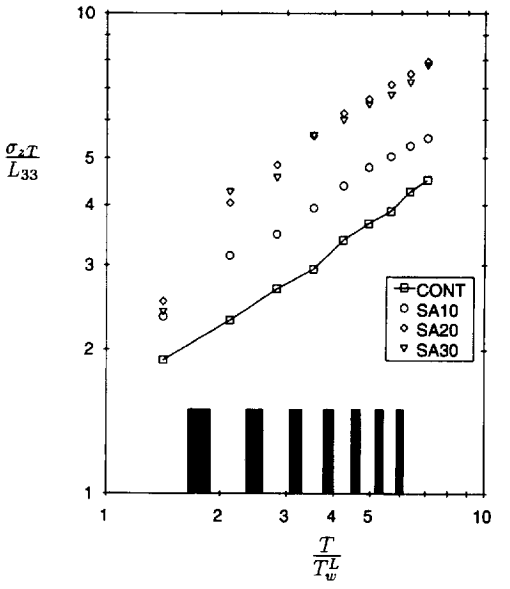

Fig. 17. The effects of changes in the array height on the vertical extent (at $y/W = 0$) of a plume passing through the staggered array [CAMB].

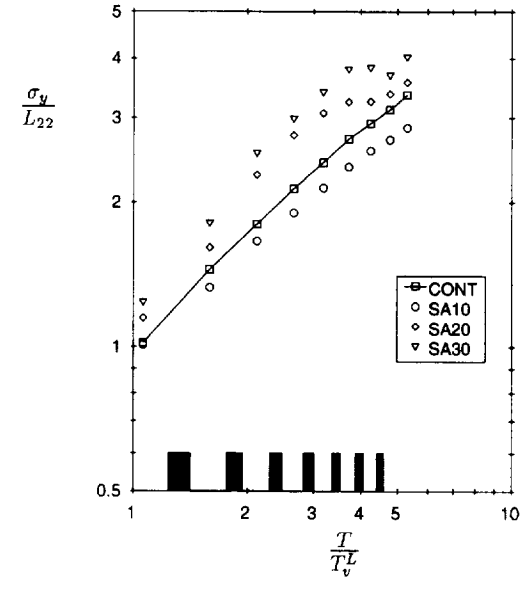

Fig. 16. The effects of changes in the array height on the lateral width (at $z = H/2$) of a plume passing through the staggered array [CAMB].

dispersion of the plume. With this limited amount of data and no flow-field data within the arrays, it is difficult to draw conclusions. The data do indicate that the plume behaviour is sensitive to the height of the obstacles and that further detailed investigations are required.

3.2.3. *Source position.* For a given set of ambient conditions the position of the source determines the size of the plume as it reaches the obstacle array. If the plume is small relative to the first obstacle it reaches then mixing in the near-wake region will increase the size of the plume to that of the obstacle. Conservation of tracer flux dictates that there must be a corresponding drop in the mean concentration. This can be seen in Figs 18–20, where the mean plume parameters are presented for three plumes: the control plume, a plume released from a source located relatively close to the array (1 B upstream) and a plume released from a source a significant distance (10B) upstream of the array. These data were obtained during the EPA experiments with the staggered array and we revert to the traditional method of scaling for simplicity. Comparing the array plume when the source is close to the array ($x_a = 1B$) with the control plume, we see a dramatic increase in the lateral and vertical spread of the plume and a corresponding drop in the mean concentration at the position of the first obstacle with which the plume interacts. When the plume is of the same order or larger than the first obstacle with which it interacts, these rapid changes in the scale and concentration of the plume are not observed. This is evident in the data from a plume released 10B upstream of the centre of the array. The changes to this plume occur gradually and these are the changes described in Section 3.2.1. It is worth noting that the expansion of the plume in the near wake of an obstacle generates a plume larger than the remaining obstacles in its path and therefore this effect will only occur once within an array of similar sized obstacles. The importance of the position of the source relative to individual obstacles is dependent on the scale of the plume relative to the first obstacle with which it interacts. The importance

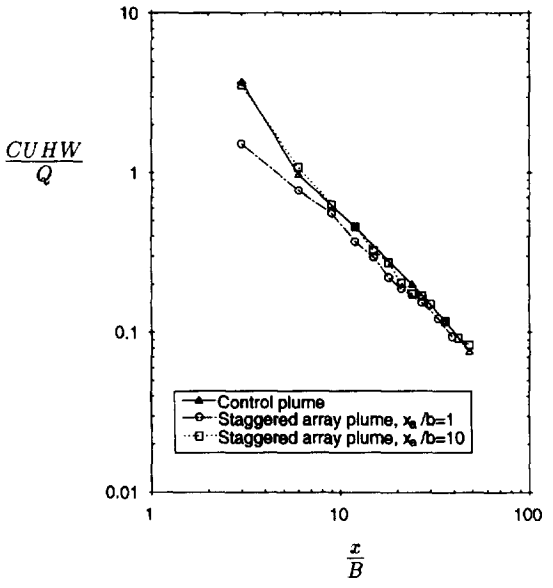

Fig. 18. The effects of changes in the source position on the decay of mean concentration (at $z = H/2$, $y/W = 0$) with downstream distance of a plume passing through the staggered array [EPA].

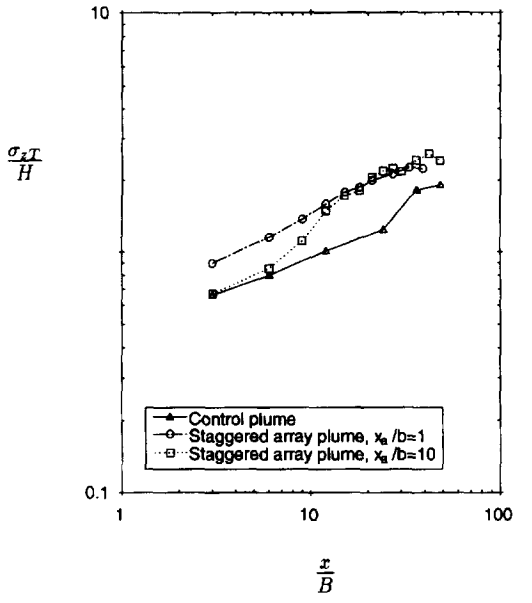

Fig. 20. The effects of changes in the source position on the vertical extent (at $y/W = 0$) of a plume passing through the staggered array [EPA].

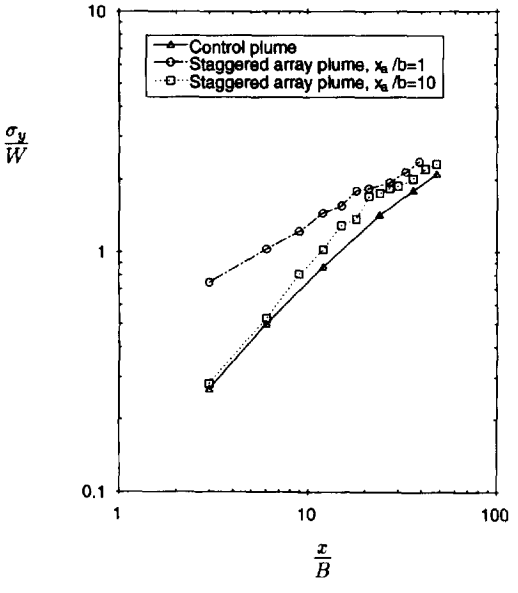

Fig. 19. The effects of changes in the source position on the lateral growth (at $z = H/2$) of a plume passing through the staggered array [EPA].

of the position of the source relative to the dividing streamline has already been discussed in Section 3.1.

4. CONCLUSIONS

Data from the wind-tunnel simulations described in this paper have increased our confidence in the conclusions drawn from the field study and they have provided experimental evidence of many of the concepts developed during the field programme. Combining the results from the detailed flow field and dispersion experiments, we can conclude that there are two mechanisms that determine the behaviour of a plume as it passes through a large group of obstacles: the divergence and convergence of streamlines as the fluid passes around the group of obstacles as a whole and the changes to the structure of the turbulence as eddies are shed from the individual obstacles. The measurements within the obstacle arrays indicate that there are only small changes in the transverse eddy diffusivities despite reductions in the scales and increases in the strength of the turbulent fluctuations. Therefore changes to the structure of the turbulence have little effect on decay of the mean concentration and the spread of the plume. The divergence of streamlines near the upstream end of a low flat obstacle array increases the overall height of the plume by approximately 50% in these experiments. The effects of the converging streamlines near the downstream end of the array are not as significant, since the streamlines converge over a much greater distance than that over which they diverge. These changes do not alter the mean structure of the plume; the mean concentration profiles have Gaussian forms as the plumes pass through the arrays.

These conclusions have been confirmed on three scales: 1:1, 1:20 and 1:200. It has also been shown that reasonable quantitative agreement between the data from the experiments, conducted at three scales, can be obtained by scaling with upstream flow field statistics and that this is superior when compared with the standard method of scaling. However, where

the plume passes into a flow field dominated by eddies shed from the obstacles, an obstacle length scale will be the most relevant scaling parameter. With the appropriate scaling, wind tunnels with a simulated atmospheric boundary layer are able to reproduce the results of full-scale situations and useful results can be obtained with small wind tunnels, such as the one at Cambridge.

In addition to comparisons with the field data, we were able to extend the wind-tunnel simulations to consider how changes in some parameters influence the behaviour of the plumes. The position of the source relative to the array, for example, determines the proportions of the plume that will pass into and over the array and the size of the plume at the point of initial interaction with an obstacle within the array. If the plume is large relative to the obstacle then only the local structure of the plume and the concentration fluctuations are affected. If, however, the plume is small relative to the obstacle, mixing in the near wake of the obstacle increases the size of the plume to that of the obstacle and thus there are dramatic changes to the extent, dilution and structure of the plume. A number of small-scale experiments (1 : 200) indicates that the configuration of the obstacle array is significant where the rows of the obstacles present channels to the flow. These channels restrict the lateral growth of the plume. These experiments also showed that the *effective gap* between the obstacles (as they would appear to an upstream observer) is inversely correlated with the increase in the vertical height of the plume and that the results are sensitive to the height of the array.

Clearly, more research is required, particularly with respect to the flow field, before we can be confident that we understand the behaviour of a plume passing through a large array of obstacles, but through these studies we have been able to develop some general concepts which can be applied when presented with such a problem.

Acknowledgements—The authors would like to acknowledge the financial support of the U.K. Ministry of Defence. The first author would also like to thank the Hong Kong University of Science and Technology for the use of their facilities when preparing this paper.

Disclaimer—The information in this document has been funded in part by the United States Environmental Protection Agency. It has been subjected to Agency review and approved for publication. Mention of trade names or commercial products does not constitute endorsement or recommendation for use.

REFERENCES

Bradbury L. J. S and Castro I. P. (1971) A pulsed-wire technique for velocity measurements in highly turbulent flows. *J. Fluid. Mech.* **49,** 657–691.

Britter R. E. and Hunt J. C. R. (1979) Velocity measurements and order of magnitude estimates of the flow between two buildings in a simulated atmospheric boundary layer. *J. Ind. Aero.* **3,** 165–182.

Britter R. E., Hunt J. C. R. and Mumford J. C. (1979) The distortion of turbulence by a circular cylinder. *J. Fluid Mech.* **92,** 269–301.

Castro I. P. and Robins A. G. (1977) The flow around a surface mounted cube in uniform and turbulent streams. *J. Fluid Mech.* **79,** 307–335.

Castro I. P. and Snyder W. H. (1982) A wind tunnel study of dispersion from sources downwind of three-dimensional hills. *Atmospheric Environment* **16**(8), 1869–1887.

Cermak J. E., Lombardi D. J. and Thompson R. S. (1974) Applications of physical modelling to the investigations of air pollution problems in urban areas. Paper No. 74–160, 67th annual meeting of the Air Pollution Control Association, Denver, Colorado.

Counihan J. (1969) An improved method of simulating an atmospheric boundary layer in a wind tunnel. *Atmospheric Environment* **3,** 197–214.

Davidson M., Mylne K., Jones C., Phillips J., Perkins R., Fung J. and Hunt J. C. R. (1995) Plume dispersion and large groups of obstacles — a field investigation. *Atmospheric Environment* **29**(22), 3245–3256.

Davies M. E., Quincey V. G. and Tindall S. J. (1980) The near wake of a tall building block in uniform and turbulent flows. In *Proc. 5th Int. Conf. on Wind Engineering*, Vol. 1 (Cermak), Ft. Collins, Colorado, pp. 289–298. Pergamon Press, New York.

Fackrell J. E. (1984) An examination of simple models for building influenced dispersion. *Atmospheric Environment* **18,** 89–98.

Hosker R. (1981) Methods for estimating wake flow and effluent dispersion near simple block-like buildings. NOAA technical memorandum ERL ARL-108, Air Resources Laboratories, Silver Spring, Maryland.

Hosker R. and Pendergrass W. R. (1987) Flow and dispersion near clusters of buildings. NOAA Technical Memorandum ERL ARL-153, Air Resources Laboratories, Silver Spring, Maryland.

Hunt J. C. R. (1984) Flow around bluff obstacles. Lecture notes, Von Karman Institute, Brussels.

Hunt J. C. R. (1985) Turbulent diffusion from sources in complex flows. *Ann. Rev. Fluid Mech.* **17,** 447–485.

Hunt J. C. R. and Mulhearn P. J. (1973) Turbulent dispersion from sources near two-dimensional obstacles. *J. Fluid Mech.* **61,** 245–274.

Jacko R. B., Palmer G. M. and Brenchley D. L. (1972) A wind tunnel study to determine the air pollution dispersion characteristics in an urban center, 65th annual meeting of the Air Pollution Control Association, Miami Beach, Florida.

Jerram N., Perkins R., Fung J., Davidson M., Belcher S. and Hunt J. C. R. (1995) Atmospheric flow through groups of buildings and dispersion from localised sources. In *Wind Climate and Cities* (edited by Cermak J. E.), pp. 109–130. Kluwer Academic Publishers, Dordrecht.

Jones C. D. and Griffiths R. F. (1984) Full-scale experiments on dispersion around an isolated building using an ionized air tracer technique with very short averaging time. *Atmospheric Environment* **18,** 903–916.

Kim S., Brandt H. and White B. R. (1990) An experimental study of two dimensional atmospheric gas dispersion near two objects. *Boundary-Layer Met.* **52,** 1–16.

Pasquill F. and Smith F. B. (1983) *Atmospheric Diffusion*, 3rd Edn, Ellis Horwood, Chichester.

Puttock J. S. and Hunt J. C. R. (1979) Turbulent diffusion from sources near obstacles with separated wakes, Part 1: An eddy diffusivity model. *Atmospheric Environment* **13,** 1–13.

Snyder W. H. (1992) Some observations of the influence of stratification on diffusion in building wakes. IMA Conf. on Stably Stratified Flows, University of Surrey, Guildford, England.

Snyder W. H. (1993) Downwash of plumes in the vicinity of buildings a wind-tunnel study. In *Proc. NATO Advanced Research Workshop: Recent Advances in the Fluid Mechanics of Jets and Plumes*, Viana do Castelo, Portugal.

Snyder W. H., Davidson M. J. and Lawson R. E. Jr. (1991) Building Array-Neutral Plumes. In *Fluid Modeling Facility Internal Report*, United States Environmental Protection Agency, North Carolina.

Snyder W. H. and Lawson R. E. Jr. (1994) Wind-tunnel measurements of flow fields in the vicinity of buildings, 8th AMS Conf. on Appl. Air Poll. Meteorol., with AWMA, Nashville, Tennessee.

Turfus C. (1986) Diffusion from a continuous source near a surface in steady reversing shear flow. *J. Fluid Mech.* **172,** 183–209.